biomedicines

MDPI

Article

Development and Validation of a Novel Oral Orotracheal Bronchoalveolar Lavage Device for Improved Bronchoalveolar Lavage in Mice

Mujie Zhang [1], Jiacheng Deng [1], Wenxin Ji [1], Xiaoyan Tian [2], Leyao Liang [1], Yingjun Li [2], Zhenyu Liao [3], Liang Peng [1,2,*] and Jianhua Li [1,3,*]

[1] KingMed School of Laboratory Medicine, Guangzhou Medical University, Guangzhou 511436, China; zmj_980817@126.com (M.Z.); tuzrboss16@gmail.com (J.D.); 13434902719@163.com (W.J.); 13005865900@163.com (L.L.)
[2] Key Laboratory of Biological Targeting Diagnosis, Therapy and Rehabilitation of Guangdong Higher Education Institutes, The Fifth Affiliated Hospital, Guangzhou Medical University, Guangzhou 510700, China; txy_010908@126.com (X.T.); lyj990109@163.com (Y.L.)
[3] China-Portugal Belt and Road Joint Laboratory on Artificial Intelligence and Public Health Issues, School of Basic Medical Sciences, Guangzhou Medical University, Guangzhou 511436, China; 19914669155@163.com
* Correspondence: pl_206@126.com (L.P.); lijianh@gzhmu.edu.cn (J.L.)

Abstract

Background: Bronchoalveolar lavage (BAL) is widely used to assess pulmonary inflammation, but conventional tracheotomy-based lavage (TBL) requires tracheal incision, cannulation, and fixation and may contribute to procedural trauma and blood contamination. We developed a novel oral orotracheal bronchoalveolar lavage device (OOBL) and evaluated its procedural performance, bronchoalveolar lavage fluid (BALF) quality, and recovery of inflammatory readouts. **Methods**: Thirty-two female C57BL/6J mice ($n = 8$ per group) received oropharyngeal instillation of PBS or lipopolysaccharide (LPS; 5 mg/kg) and underwent BAL 12 h later using TBL or OOBL. Operating time, procedural success, and BALF recovery were assessed together with BALF cell counts, protein, flow cytometry, and ELISA; lung histology and qRT-PCR were used to validate the inflammatory model. **Results**: OOBL shortened operating time (3.9 ± 0.7 vs. 8.7 ± 1.2 min) and increased BALF recovery ($88.5 \pm 4.0\%$ vs. $64.4 \pm 18.8\%$). Under PBS conditions, OOBL yielded lower BALF red blood cell counts and protein concentrations than TBL. Under LPS-induced inflammatory conditions, OOBL yielded higher BALF MPO, IL-1β, and TNF-α, with a trend towards higher total and white blood cell counts, whereas IL-6 did not differ between lavage methods. **Conclusions**: OOBL eliminates tracheal incision, catheter insertion through the tracheal incision, and suture fixation, although a limited cervical incision and tracheal exposure are still required for visual confirmation of placement. These preliminary findings suggest that OOBL may be an efficient and reproducible BAL device for murine pulmonary research, although further validation is warranted.

Keywords: bronchoalveolar lavage; oral orotracheal bronchoalveolar lavage device; mouse model; acute lung injury; inflammatory assessment

Check for updates

Academic Editor: Alberto Ricci

Received: 4 September 2026
Revised: 9 October 2026
Accepted: 14 October 2026
Published: 18 November 2026

Copyright: © 2026 by the authors. Licensee MDPI, Basel, Switzerland. This article is an open access article distributed under the terms and conditions of the Creative Commons Attribution (CC BY) license.

1. Introduction

Bronchoalveolar lavage (BAL) is an essential technique for studying pulmonary diseases and evaluating local immune responses and inflammatory status [1–3]. In mouse models, bronchoalveolar lavage fluid (BALF) is widely used to measure inflammatory cell

recruitment, cytokine expression, and alveolar barrier function [4–6]. Currently, the most common BAL procedure in mice is tracheotomy-based lavage (TBL), which requires cervical surgery including tracheal exposure, incision, cannulation, and suture fixation [7–9]. This multi-step process is time-consuming and demands high technical skill [10–12]. The rich vascular supply and complex cervical anatomy increase the risk of local tissue and vessel injury [13,14], leading to blood contamination that compromises BALF quality and assay sensitivity [15,16]. Luckow et al. described an orotracheal intubation method using a commercially available "olive-tip metal cannula" to bypass tracheotomy. However, this approach lacks customised optimisation for BAL and has not been systematically evaluated for sample quality and inflammatory detection [15]. More recently, a transoral endotracheal intubation method using a combination of commercial equipment has been proposed, yet it still relies on auxiliary devices such as laryngoscopes, microscopes, and intubation platforms, making the procedure relatively complex [17]. Therefore, there is a clear need for a dedicated BAL device that is simple, reproducible, and suitable for standardised use [18,19], simplifying the procedure by eliminating tracheal incision and suture fixation.

In this study, we developed a novel oral orotracheal bronchoalveolar lavage device (OOBL) and systematically compared its performance with TBL in terms of operational efficiency, BALF quality, and inflammatory detection sensitivity using a lipopolysaccharide (LPS)-induced acute lung injury model [20–22]. We also discuss its potential for simplifying the procedure, optimising experimental workflow, and alignment with the 3Rs principles (Replacement, Reduction, Refinement) [23]. We hypothesised that, compared with conventional tracheotomy-based lavage, the OOBL would reduce procedural complexity and operating time, improve BALF recovery and sample quality, and enhance the recovery of BALF-associated inflammatory readouts in mice.

2. Materials and Methods

2.1. Study Design

A 2 × 2 factorial study design compared treatment (PBS versus LPS) and lavage method (TBL versus OOBL). Thirty-two female C57BL/6J mice were allocated to four groups ($n = 8$ per group): PBS-TBL, PBS-OOBL, LPS-TBL, and LPS-OOBL. The experimental unit was the individual mouse. Twelve hours after oropharyngeal PBS or LPS instillation, BAL was performed using the assigned method, followed by BALF and lung tissue analyses.

2.2. Sample Size

Thirty-two mice were used in total, with 8 animals allocated to each of the four experimental groups. The sample size was determined based on previous studies using comparable murine BAL and LPS-induced lung inflammation models, together with our preliminary experimental experience, while considering the Reduction principle of the 3Rs. A formal a priori power calculation was not performed.

2.3. Inclusion and Exclusion Criteria

No animals were excluded from the study after group allocation, and all 32 mice were included in the final analyses. Procedural failure was defined a priori as the inability to complete all three planned instillation-aspiration cycles. Two mice in the TBL groups completed only one instillation-aspiration cycle and were therefore classified as procedural failures; however, the BALF obtained from these mice was retained and included in subsequent analyses. No data points were excluded as outliers.

2.4. Randomization

The 32 mice were individually numbered and randomly allocated to four experimental groups (PBS-TBL, PBS-OOBL, LPS-TBL, and LPS-OOBL; $n = 8$ per group) using a random number method.

2.5. Blinding

Blinding was not feasible during the BAL procedures because the TBL and OOBL techniques were visually and operationally distinct; therefore, the investigator performing BAL was aware of group allocation. After sample collection, all samples and histological sections were coded, and investigators performing BALF analyses, flow cytometry, ELISA, histopathological assessment, and qRT-PCR were blinded to group allocation. Group identities were revealed only after outcome assessment was completed.

2.6. Outcome Measures

The principal outcome measures for evaluating lavage performance were operating time, procedural success rate, and BALF recovery rate. Additional outcome measures were used to assess BALF sample quality and inflammatory readout recovery, including total cell count (TC), white blood cell count (WBC), red blood cell count (RBC), protein concentration, the proportion of $CD11b^{+}Ly6G^{+}$ neutrophils, and BALF concentrations of myeloperoxidase (MPO), interleukin-1β (IL-1β), tumour necrosis factor-α (TNF-α), and interleukin-6 (IL-6). Lung histopathology and lung tissue expression of IL-1β, TNF-α, and IL-6 mRNA were assessed to confirm the establishment of LPS-induced pulmonary inflammation rather than as measures of lavage performance.

2.7. Experimental Animals

Thirty-two specific-pathogen-free (SPF) female C57BL/6J mice, aged 6–8 weeks and weighing 18–22 g, were obtained from Beijing Vital River Laboratory Animal Technology Co., Ltd. (Beijing, China). Animals were housed in the SPF barrier facility of the Laboratory Animal Center of Guangzhou Medical University and were acclimatised for 3 days before the experiments. The animal room was maintained on a 12 h light/12 h dark cycle at approximately 20–26 °C and 50–70% relative humidity, with adequate ventilation and a noise level below 60 dB. Bedding was changed regularly, and the housing environment was routinely sanitised. Standard laboratory chow and water were provided ad libitum.

2.8. Reagents and Materials

LPS (E. coli O111:B4, L2630; Sigma-Aldrich, St. Louis, MO, USA) and mouse Fc receptor blocker (abs-9477; Absin, Shanghai, China) were used. Zombie Aqua™ Fixable Viability Kit (423101), FITC anti-mouse Ly6G antibody (127605, clone 1A8), and APC anti-mouse/human CD11b antibody (101211, clone M1/70) were from BioLegend (San Diego, CA, USA). Mouse IL-6 (EK0411), IL-1β (EK0394), TNF-α (EK0527), and MPO (EK0943) ELISA kits were from BOSTER (Pleasanton, CA, USA). OOBL devices were custom-made from polypropylene.

2.9. LPS-Induced Acute Lung Injury

Mice were anaesthetised with intraperitoneal Avertin (tribromoethanol, 1.25% ready-to-use solution, Dalian Meilun Biotechnology, Dalian, China, MA1612) at a dose of 17–20 μL/g body weight (approximately 212–250 mg/kg). Adequate anaesthesia was confirmed by the absence of a pedal withdrawal reflex and a stable respiratory rate. The mice were placed on an intubation platform. PBS or LPS (5 mg/kg in 50 μL) was instilled oropharyngeally using a pipette, followed by gentle closure of the nostrils for approximately 10 s and upright

holding to facilitate aspiration. The mice were then gently returned to their cages and maintained for 12 h before subsequent procedures.

2.10. Bronchoalveolar Lavage and Sample Collection

After anaesthesia, a 1.0 cm midline cervical incision was performed, and subcutaneous tissues were bluntly dissected to expose the tracheal rings without incision. For OOBL, the device was attached to a 1 mL syringe, inserted orally along the palate, and advanced until the tip was visualised in the tracheal lumen through the exposed cervical window. Successful placement was confirmed by direct visualisation of the tip within the mid-trachea. The hand-grip was then secured at the oral commissure, which served as a stop to standardise the insertion depth at 25 mm across animals. All lavage procedures were performed by a single experienced operator who had completed at least 20 training procedures in mice. Pre-chilled PBS (500 µL) was slowly instilled, held for 30 s, and aspirated; this was repeated three times (total 1.5 mL). The BALF recovery rate was calculated as (volume of BALF recovered/total volume of PBS instilled) × 100%. For TBL, a small incision was made between tracheal rings, a 24-gauge intravenous catheter was inserted and fixed with a suture, and the same lavage protocol was applied. BALF was kept on ice.

2.11. BALF Cell Counting

Total cell, white blood cell, and red blood cell counts were determined using an automated haematology analyser (BC-7500 CS; Mindray, Shenzhen, China) in body fluid mode.

2.12. Flow Cytometry

Cells from BALF were pelleted by centrifugation at 400× *g* for 5 min at 4 °C and resuspended in FACS buffer. For live/dead cell discrimination, cells were incubated with Zombie Aqua™ Fixable Viability Kit (1:1000 dilution) at room temperature for 15 min in the dark. After washing, cells were blocked with mouse Fc receptor blocker (0.5 µg per 10^6 cells) for 10 min and then stained with APC anti-mouse/human CD11b (0.25 µg per 10^6 cells) and FITC anti-mouse Ly6G (0.25 µg per 10^6 cells) antibodies for 20 min at room temperature in the dark. Following two washes with FACS buffer, stained cells were resuspended in FACS buffer and analysed on a BD FACSCanto II flow cytometer (BD Biosciences, Franklin Lakes, NJ, USA). Compensation was performed using single-stained and unstained controls. A minimum of 10,000 events per sample were acquired. Data were analysed using FlowJo software v10.0 (BD Biosciences, Franklin Lakes, NJ, USA).

2.13. ELISA

BALF supernatants were assayed for IL-6, IL-1β, TNF-α, and MPO using commercial ELISA kits according to the manufacturer's instructions.

2.14. Lung Histopathology

Left lung lobes were fixed in 4% paraformaldehyde for 24 h, dehydrated, paraffin-embedded, sectioned, and stained with haematoxylin and eosin (H&E) for histological examination.

2.15. qRT-PCR

Total RNA was extracted from right lung tissues using a commercial RNA extraction kit (400–100, Goonie, Guangzhou, China) according to the manufacturer's instructions. Reverse transcription was performed using the Fast First-Strand cDNA Synthesis Mix for RT (with dsDNase) kit (500–101, Goonie, Guangzhou, China). Briefly, 1000 ng of total RNA was used in a 20 µL reaction volume, and the two-step protocol included genomic DNA

removal at 37 °C for 2 min and 65 °C for 2 min, followed by reverse transcription at 50 °C for 15 min and 85 °C for 5 min. mRNA levels of *IL-6*, *IL-1β*, and *TNF-α* were quantified by qRT-PCR with *β-actin* as an internal control, and primer sequences and amplicon sizes are listed in Supplementary Table S1. Relative mRNA expression was calculated using the $2^{-\Delta\Delta Ct}$ method.

2.16. Statistical Methods

Data are expressed as mean ± SD. Normality was assessed using the Shapiro-Wilk test. For BALF TC, WBC, and RBC counts and protein concentration obtained from the 2 × 2 factorial design, data were $\log_{10}$-transformed before analysis to improve conformity with the assumptions of parametric analysis. The effects of treatment (PBS vs. LPS), lavage method (TBL vs. OOBL), and their interaction were evaluated using ordinary two-way ANOVA. When appropriate, comparisons between TBL and OOBL within each treatment condition were performed using Šídák's multiple comparisons test. For all other continuous variables (operating time, BALF recovery rate, neutrophil percentage, cytokine concentrations, and mRNA expression), an unpaired *t* test was used for normally distributed data, and the Mann-Whitney *U* test was used for non-normally distributed data. Fisher's exact test was used for categorical variables (operation success rate). A p value < 0.05 was considered statistically significant. All analyses were performed using GraphPad Prism 10.0 (GraphPad Prism Software, San Diego, CA, USA).

3. Results

3.1. Structural Design and Operation of the OOBL

Figure 1a shows the structural design of the OOBL. The device has a total length of 31.8 mm and an effective insertion length of approximately 25 mm. During use, the insertion depth is limited by a integrated hand-grip, ensuring that the tip is consistently positioned within the mid-trachea. Previous work suggests that an insertion depth of 18–20 mm is sufficient for stable intubation in mice weighing 17–25 g [24]. The OOBL tip is a spherical blunt end with an outer diameter of 1.2 mm and an inner diameter of 0.32 mm. Given that the mouse tracheal inner diameter is approximately 1 mm [25], the 1.2 mm outer diameter of the blunt tip slightly exceeds the tracheal lumen, facilitating a snug fit that may reduce fluid leakage during lavage. However, the degree of tracheal distension and any associated tissue effects were not directly assessed in this study. The 0.32 mm inner diameter was selected to allow adequate fluid exchange while potentially limiting mechanical stress on cells.

Figure 1b presents the physical device made of polypropylene (PP), which is autoclavable, reusable, and low-cost. An integrated hand-grip in the middle facilitates stable handling and directional control. After oral insertion, the grip rests against the oral commissure, fixing the insertion depth and minimising operator variability. Figure 1c illustrates the procedure: anaesthetised mice are placed supine, and the device is gently inserted along the palate; the tracheal lumen can be directly visualised through a small cervical incision (without tracheotomy) to confirm placement.

3.2. Experimental Design and BALF Collection Workflow

The operational procedures for the two lavage methods are illustrated in Figure 2a. TBL requires surgical exposure of the trachea, followed by tracheal incision, cannulation, and suture fixation. The OOBL is inserted orally with the integrated hand-grip secured at the oral commissure to control insertion depth, eliminating the need for tracheal incision, catheter insertion through the tracheal incision, and suture fixation, although a small cervical incision and tracheal exposure are still required for visual confirmation of intubation.

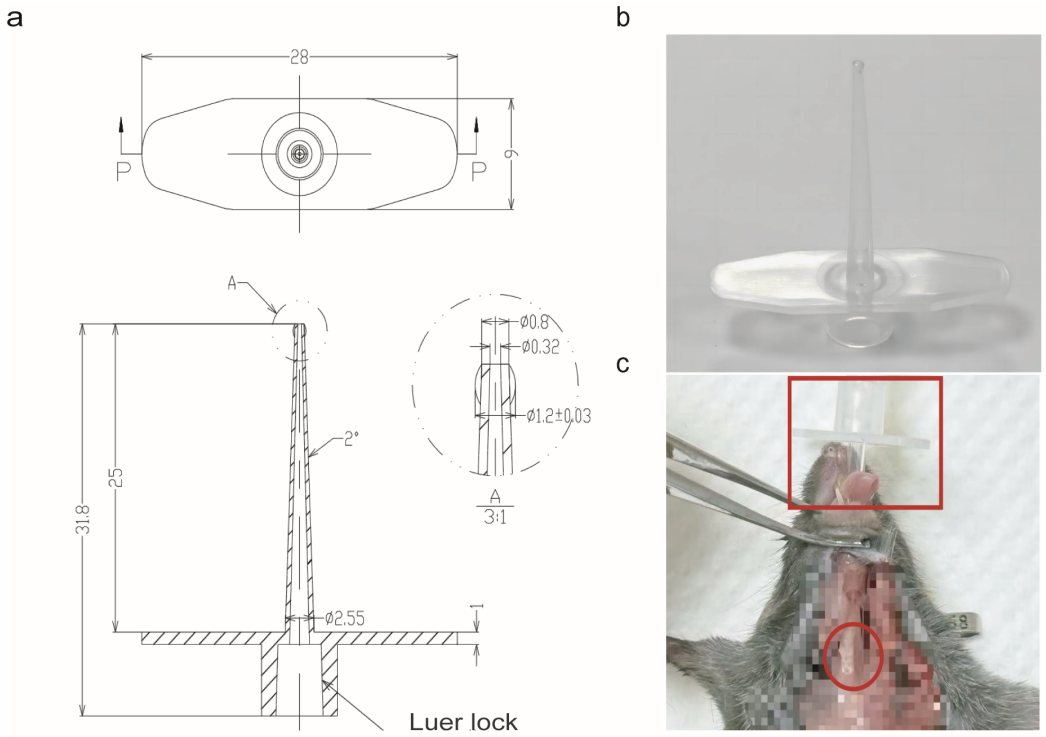


Figure 1. Structural design and operation of the OOBL. (**a**) Schematic of OOBL with dimensions and tip parameters (mm). The symbol "Ø" indicates diameter, and "2°" indicates the taper angle. "P" denotes the section plane, and "A" denotes the enlarged detail view of the tip (magnified at 3:1). (**b**) Photograph of the OOBL. (**c**) Diagram of oral insertion and BAL procedure. The red box indicates the oral insertion route. The red circle marks the position of the blunt tip after successful insertion into the mid-trachea, as visualised through the cervical window.

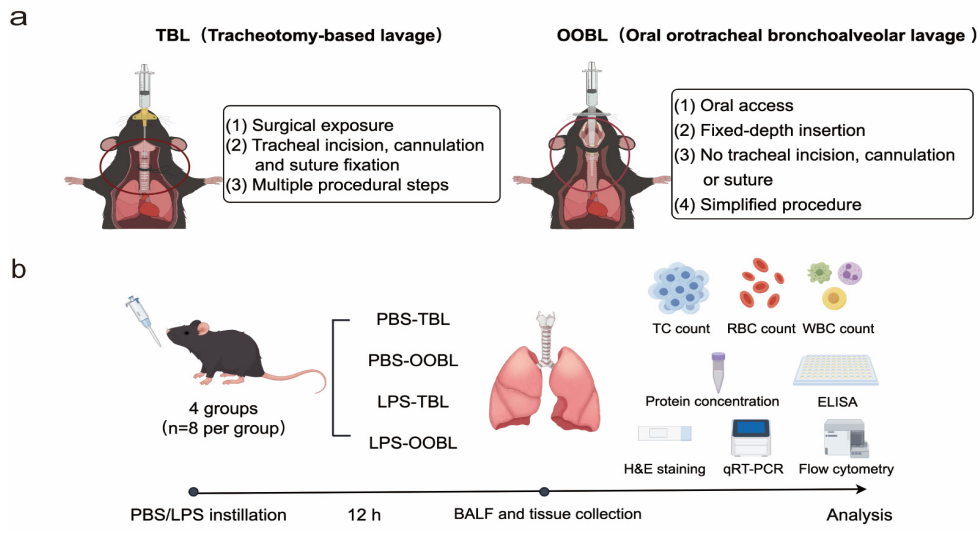


Figure 2. Experimental design and BALF collection workflow. (**a**) Schematic comparison of TBL and OOBL. TBL requires surgical exposure, tracheal incision, cannulation, and suture fixation. OOBL uses oral access with fixed-depth insertion, eliminating the need for tracheal incision, cannulation, and suture fixation. (**b**) Mouse groups, treatment timeline, and collected samples for subsequent analyses. Schematic created using Figdraw (https://www.figdraw.com/, accessed on 18 November 2026).

Thirty-two mice were randomly assigned to four groups ($n = 8$ per group): PBS-TBL, PBS-OOBL, LPS-TBL, and LPS-OOBL. Twelve hours after oropharyngeal instillation of PBS

or LPS, BALF was collected using either TBL or OOBL, and lung tissues were harvested immediately thereafter. BALF was used for TC count, WBC count, RBC count, protein concentration, flow cytometry, and ELISA. Lung tissues were processed for H&E staining and qRT-PCR analysis (Figure 2b).

3.3. OOBL Improves Operational Efficiency and BALF Recovery

We compared TBL and OOBL in terms of operating time, success rate, and BALF recovery. OOBL markedly shortened the procedure time (3.9 ± 0.7 min vs. 8.7 ± 1.2 min, $p < 0.0001$) and increased the recovery rate (88.5 ± 4.0% vs. 64.4 ± 18.8%, $p < 0.0001$). The success rate was 100% for OOBL and 87.5% for TBL, with no statistically significant difference between the two methods (Table 1). These results indicate that OOBL demonstrated a high procedural success rate while significantly shortening procedure time and improving BALF recovery rate.

Table 1. Comparison of BAL procedure efficiency and BALF recovery between TBL and OOBL methods.

Lavage Method	Operating Time (min)	BALF Recovery Rate (%)	Operation Success Rate, n/N (%)
TBL	8.7 ± 1.2	64.4 ± 18.8	14/16 (87.5%)
OOBL	3.9 ± 0.7 ****	88.5 ± 4.0 ****	16/16 (100%)

Data are presented as mean ± SD ($n = 16$ per group) for continuous variables (operating time and BALF recovery rate), with data pooled across PBS and LPS conditions; operation success rate is presented as n/N (%). Statistical significance for operating time and BALF recovery was determined by the Mann-Whitney *U* test (**** $p < 0.0001$, OOBL vs. TBL). Comparison of success rates was performed using the two-sided Fisher's exact test, with $p = 0.48$ (not significant).

3.4. Establishment and Validation of the LPS-Induced Acute Lung Injury Model

To validate the inflammatory model, we comprehensively analysed BALF and lung tissues from PBS- and LPS-treated mice. Compared with the PBS group, the LPS group showed significant increases in BALF TC ($p < 0.0001$), WBC ($p < 0.0001$) and RBC ($p < 0.001$) counts, as well as protein concentration ($p < 0.001$) (Table 2). These results suggest that LPS induced substantial inflammatory cell recruitment to the alveolar space, accompanied by increased alveolar-capillary barrier permeability and erythrocyte extravasation.

Table 2. Comparison of BALF cellular composition and protein concentration between PBS and LPS groups.

Group	TC ($\times 10^6$ Cells/mL)	WBC ($\times 10^6$ Cells/mL)	RBC ($\times 10^6$ Cells/mL)	Protein Concentration (mg/mL)
PBS	101.3 ± 70.9	95.8 ± 69.8	1563.0 ± 629.2	0.2 ± 0.2
LPS	1043.0 ± 472.2 ****	1025.0 ± 466.8 ****	4125.0 ± 2964.0 ***	0.4 ± 0.2 ***

Data are presented as mean ± SD ($n = 16$ per group). *** $p < 0.001$, **** $p < 0.0001$, LPS vs. PBS.

H&E staining (Figure 3a) revealed intact pulmonary architecture with thin and uniform alveolar septa in the PBS group, whereas the LPS group exhibited marked alveolar septal thickening, extensive inflammatory cell infiltration into the interstitium and alveolar spaces, and focal alveolar disruption with intra-alveolar exudates. These morphological changes were consistent with the elevated TC and WBC counts and protein concentration in BALF.

Flow cytometry was performed to quantify $CD11b^+Ly6G^+$ neutrophils in BALF. The gating strategy sequentially excluded debris and doublets and selected live cells (Zombie $Aqua^-$) before analysing the $CD11b^+Ly6G^+$ double-positive population (Figure 3b). Representative plots (Figure 3c) and quantitative analysis (Figure 3d) showed that the percentage

of neutrophils in BALF was significantly higher in the LPS group than in the PBS group ($p < 0.0001$), indicating substantial pulmonary neutrophil infiltration in response to LPS.

qRT-PCR analysis (Figure 3e–g) demonstrated that mRNA expression levels of *IL-6*, *IL-1β*, and *TNF-α* in lung tissues were significantly upregulated in the LPS group compared with the PBS group (*IL-6*: $p < 0.0001$; *IL-1β*: $p < 0.0001$; *TNF-α*: $p < 0.001$), consistent with the inflammatory cell infiltration in BALF and the histological changes in lung tissues.

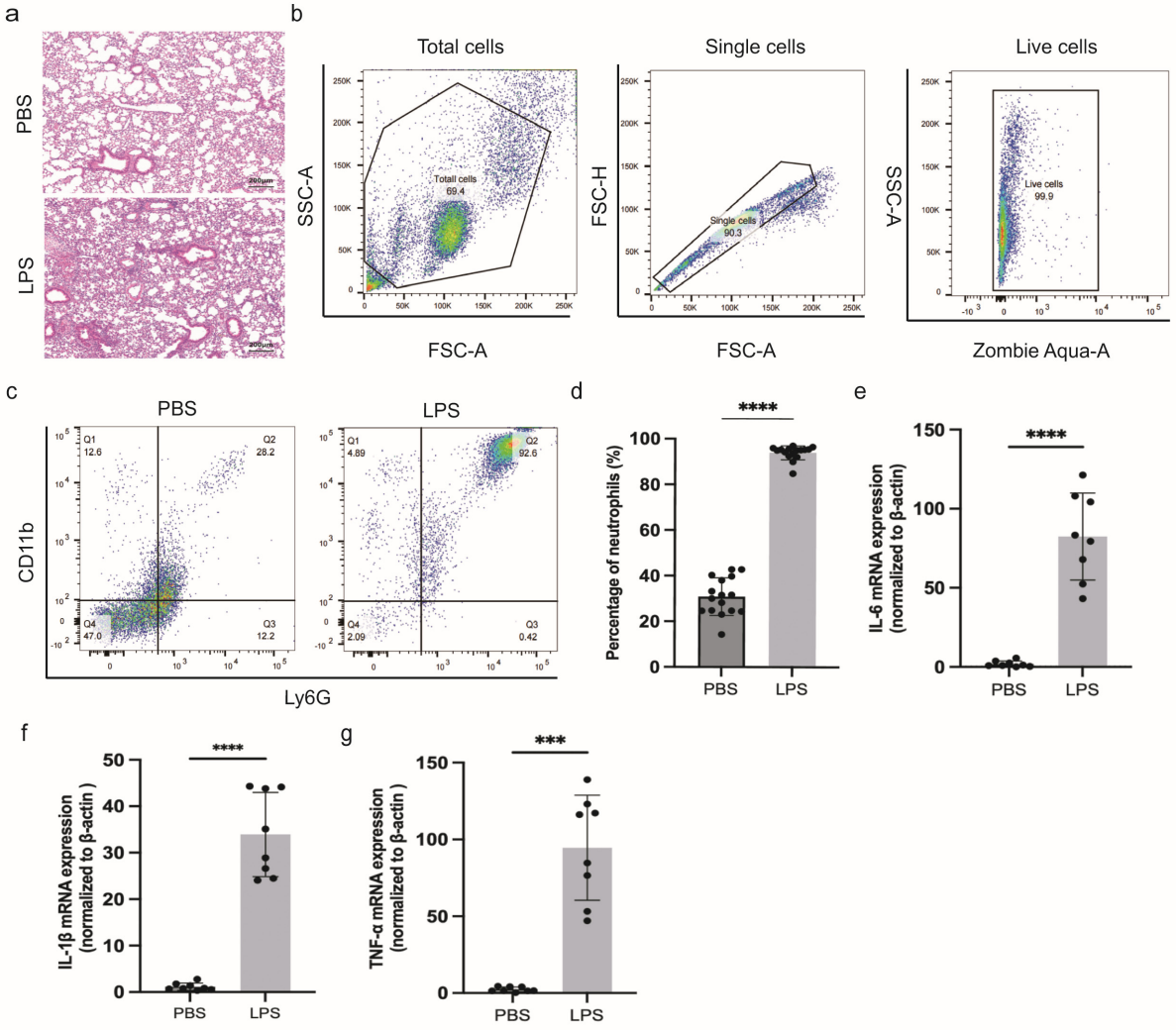


Figure 3. Validation of the LPS-induced acute lung injury model. (**a**) Representative H&E staining of lung sections from PBS and LPS groups. Scale bar: 200 μm. (**b**) Flow cytometry gating strategy for BALF neutrophils: total cells (FSC-A/SSC-A), single cells (FSC-A/FSC-H), live cells (Zombie Aqua-A/SSC-A), and $CD11b^+Ly6G^+$ double-positive population. (**c**) Representative flow cytometry plots of $CD11b^+Ly6G^+$ neutrophils in BALF from PBS and LPS groups. (**d**) Quantification of neutrophil percentage in BALF ($n = 16$ per group). (**e**–**g**) Relative mRNA expression of *IL-6*, *IL-1β*, and *TNF-α* in lung tissues, normalised to *β-actin*. Data are presented as mean ± SD ($n = 8$ per group). *** $p < 0.001$, **** $p < 0.0001$ LPS vs. PBS.

Collectively, these results confirm that LPS successfully induced an acute lung injury model characterised by neutrophil infiltration, alveolar barrier disruption, and pro-inflammatory cytokine overexpression, providing a reliable experimental foundation for subsequent comparisons of lavage methods.

3.5. OOBL Differentially Affects BALF Cell and Protein Recovery Under Physiological and Inflammatory Conditions

To evaluate whether the effects of the lavage method differ by inflammatory status, we compared BALF obtained by TBL and OOBL following PBS or LPS treatment using a two-way ANOVA design. Descriptive statistics are presented in Table 3, and the factorial analysis results are presented in Table 4.

Under PBS conditions, TC and WBC counts were comparable between the two methods. In contrast, OOBL yielded significantly lower RBC counts ($p < 0.05$) and protein levels ($p < 0.01$) compared with TBL (Tables 3 and 4).

Table 3. Comparison of BALF cellular composition and protein concentration among experimental groups.

Group	TC ($\times 10^6$ Cells/mL)	WBC ($\times 10^6$ Cells/mL)	RBC ($\times 10^6$ Cells/mL)	Protein Concentration (mg/mL)
PBS-TBL	106.1 ± 90.6	100.3 ± 89.7	2000.0 ± 534.5	0.3 ± 0.2
PBS-OOBL	96.5 ± 50.1	91.3 ± 48.4	1125.0 ± 353.6	0.1 ± 0.0
LPS-TBL	736.0 ± 251.1	721.3 ± 249.1	2375.0 ± 744.0	0.2 ± 0.1
LPS-OOBL	1351.0 ± 446.0	1329.0 ± 440.3	5875.0 ± 3357.0	0.5 ± 0.3

Data are presented as mean ± SD ($n = 8$ per group). For statistical comparisons, see Table 4.

Table 4. Two-way ANOVA and post hoc comparisons of BALF parameters.

Parameter	Interaction *p*	Treatment *p*	Lavage Method *p*	PBS: TBL vs. OOBL [a]	LPS: TBL vs. OOBL [a]
TC	0.1846	<0.0001	0.0731	0.9244	0.0601
WBC	0.2133	<0.0001	0.0698	0.8900	0.0662
RBC	0.0001	<0.0001	0.4766	0.0244	0.0019
Protein concentration	<0.0001	<0.0001	0.6170	0.0026	0.0160

[a] Šídák-adjusted *p*-value. Data were $\log_{10}$-transformed before statistical analysis. *p* values for interaction, treatment, and lavage method effects were obtained using ordinary two-way ANOVA. Comparisons between TBL and OOBL within the PBS and LPS groups were performed using Šídák's multiple comparisons test. $p < 0.05$ was considered statistically significant. $n = 8$ per group.

Under LPS-induced inflammatory conditions, both methods showed elevated TC and WBC. OOBL yielded higher TC and WBC levels than TBL, although these differences did not reach statistical significance after factorial analysis (TC: $p = 0.0601$; WBC: $p = 0.0662$). Protein concentration was significantly higher in the OOBL group than in the TBL group ($p < 0.05$). In addition, RBC levels in all LPS-treated groups were higher than those in PBS controls. OOBL yielded higher RBC levels than TBL ($p < 0.01$) under inflammatory conditions.

3.6. OOBL Enhances Inflammatory Cell Recovery and Cytokine Detection in BALF

To further evaluate the impact of different lavage methods on inflammatory assessment, flow cytometry and ELISA were used to analyse inflammatory cells and cytokines in BALF.

Flow cytometry showed that the percentage of neutrophils in BALF from LPS-treated mice was significantly higher in the OOBL group than in the TBL group ($p < 0.01$) (Figure 4a,b). ELISA results further showed that concentrations of MPO, IL-1β, and TNF-α in BALF from LPS-treated mice were significantly higher in the OOBL group than in the TBL group (MPO: $p < 0.05$; IL-1β: $p < 0.001$; TNF-α: $p < 0.01$) (Figure 4c–e). In contrast, no significant difference was observed in IL-6 levels between the two groups (Figure 4f).

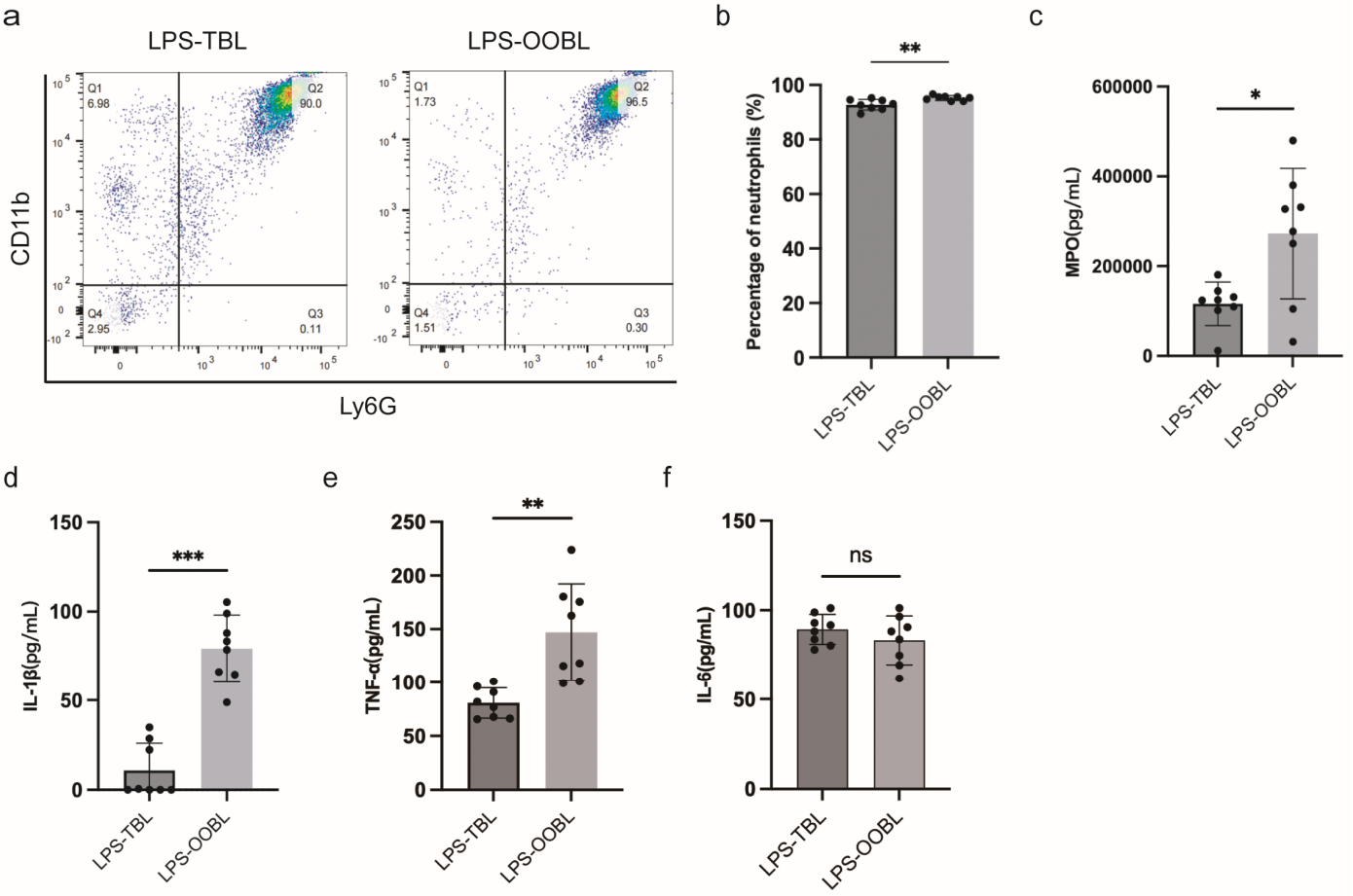


Figure 4. OOBL enhances inflammatory cell recovery and cytokine detection in BALF. (**a**) Representative flow cytometry plots of $CD11b^{+}Ly6G^{+}$ neutrophils in BALF from LPS-TBL and LPS-OOBL groups. (**b**) Quantification of neutrophil percentage in BALF. (**c**–**f**) ELISA measurements of MPO, IL-1β, TNF-α, and IL-6 in BALF. Data are presented as mean ± SD ($n = 8$ per group). * $p < 0.05$, ** $p < 0.01$, *** $p < 0.001$, OOBL vs. TBL; ns, not significant.

4. Discussion

This study presents a comprehensive evaluation of the OOBL for BAL in mice. Our results suggest that OOBL may offer significant advantages over TBL in terms of operational efficiency, sample quality, and inflammatory detection sensitivity. The OOBL incorporates three key design features that distinguish it from previously described orotracheal devices, such as the olive-tip metal cannula [15]. First, the integrated hand-grip, positioned 25 mm from the tip, standardises insertion depth across operators, minimising inter-operator variability. Second, the spherical blunt tip creates a gentle seal with the tracheal wall to reduce leakage while minimising the risk of sharp-edge injury. Third, the inner diameter (0.32 mm) is optimised to balance adequate fluid exchange with reduced mechanical shear on alveolar macrophages—a consideration less critical for devices designed primarily for ventilation. These design characteristics likely contribute to the improved BAL performance observed in this study. In addition to these structural advantages, OOBL also simplifies the procedure by eliminating tracheal incision, catheter insertion through the tracheal incision, and suture fixation.

In terms of sample quality, OOBL significantly reduced RBC contamination in BALF under control conditions and yielded higher protein concentrations under inflammatory conditions, with a trend towards higher cell counts. Under PBS conditions, OOBL yielded significantly lower RBC and protein levels in BALF compared with TBL, which may be

consistent with less procedural blood contamination. However, because tracheal injury was not directly assessed histologically, this finding should not be interpreted as definitive evidence of reduced tissue trauma. Under LPS-induced inflammatory conditions, however, OOBL yielded higher RBC levels than TBL. Since OOBL had already shown lower RBC levels under PBS conditions, the higher RBC levels in the LPS-OOBL group are more likely attributable to more efficient retrieval of extravasated erythrocytes from the inflamed alveolar space [26], rather than greater procedural injury. Nevertheless, our current data cannot definitively distinguish between RBC derived from LPS-induced vascular leakage and those from procedural microhaemorrhage; both mechanisms may contribute to the observed difference. Future studies incorporating vascular permeability assays or histological microvascular injury scoring will be necessary to clarify this issue.

From a structural design perspective, the length and tip dimensions of OOBL are optimised to position the device in the mid-trachea without deep bronchial insertion. This placement allows the lavage fluid to distribute evenly into both lungs. The spherical blunt tip, with an outer diameter slightly larger than the tracheal lumen, may help reduce fluid leakage; however, whether this degree of tracheal distension is associated with epithelial injury requires further investigation. In addition, although the inner diameter is relatively small, it remains significantly larger than the size of murine alveolar macrophages and other major cell types [27]. Gentle handling was used during all lavage procedures to minimise potential mechanical stress on cells; however, cellular integrity was not directly assessed in this study.

Regarding inflammatory detection, OOBL enhanced the recovery of MPO, IL-1β, and TNF-α. However, IL-6 levels did not differ significantly between the two methods. Although LPS stimulation markedly upregulated *IL-6* mRNA in lung tissue, its protein level in BALF may not directly reflect local transcriptional activity, as mRNA represents intracellular synthesis while BALF protein reflects secretion into the alveolar space. This discrepancy is likely attributable to multiple factors. First, different cytokines exhibit distinct patterns of local enrichment and release in BALF [28]. Second, alveolar-blood compartmentalisation and lavage fluid dilution may affect the recovery of soluble molecules [29].

Importantly, the higher cytokine levels observed in the OOBL group are more likely attributable to improved sampling rather than differences in the actual inflammatory status, as both groups received the same LPS challenge. These findings suggest that OOBL may improve the recovery of BALF-associated inflammatory readouts. However, differences in recovered volume, dilution, and procedure-related injury cannot yet be fully excluded as contributing factors. From an animal welfare perspective, OOBL eliminates the need for tracheal incision, catheter insertion through the tracheal incision, and suture fixation. Although a small cervical incision and tracheal exposure are still required for visual confirmation of intubation, OOBL reduces procedural complexity compared with TBL, which may align with the refinement principle of the 3Rs [30]. However, this study did not directly measure animal burden or reduction in animal use, and these potential benefits require further evaluation.

Several limitations warrant consideration. First, our validation was confined to an LPS-induced acute injury model; further studies are needed in infectious pneumonia, chronic inflammation, and other disease settings. Second, although OOBL avoids direct tracheal incision, a limited cervical skin incision is still required for visual confirmation of intubation, so it does not yet constitute a completely non-invasive procedure. Third, we did not perform direct histological evaluation of tracheal injury immediately following the complete OOBL or TBL procedure, including fluid instillation and aspiration, nor did we assess the mechanical consequences of using a 1.2 mm tip in a trachea with an approximate inner diameter of 1 mm, and cellular integrity following lavage was not directly evaluated. While lower

RBC counts and protein concentrations were observed in the OOBL group under PBS conditions, direct evidence of differential tissue damage between the two methods was not obtained. Fourth, the OOBL was evaluated only in female C57BL/6J mice within a relatively narrow age and body weight range, and we have not evaluated repeated lavage, longitudinal monitoring, or its application in other mouse strains or species. Because airway anatomy and dimensions may vary with strain, body size, and species, the optimal insertion depth and device dimensions should be revalidated before broader application. Future studies should further evaluate the OOBL across different disease models, mouse strains, and species, as well as in repeated or longitudinal lavage settings, together with direct assessment of tracheal injury and further device optimisation, to better define its applicability and potential value in improving animal welfare and reducing procedural stress.

5. Conclusions

In conclusion, these preliminary findings suggest that OOBL may be a reliable, efficient, and reproducible tool for improving BAL performance in mice. However, further validation in larger cohorts, different mouse strains, sexes, and disease models is needed before broader application can be recommended.

Supplementary Materials: The following supporting information can be downloaded at https://www.mdpi.com/article/10.3390/biomedicines14112670/s1, Table S1. Primer sequences and amplicon sizes used for qRT-PCR.

Author Contributions: Formal analysis, W.J., X.T. and Z.L.; investigation, M.Z., J.D., L.L. and Y.L.; resources, L.P. and J.L.; data curation, W.J., X.T. and Z.L.; writing—original draft preparation, M.Z.; writing—review and editing, M.Z., J.D., W.J., X.T., L.L., Y.L., Z.L., L.P. and J.L.; visualization, M.Z.; supervision, L.P. and J.L.; project administration, L.P. and J.L.; funding acquisition, L.P. and J.L. All authors have read and agreed to the published version of the manuscript.

Funding: This work was supported by the National Natural Science Foundation of China (Grant No. 81470205), Guangdong Provincial Natural Science Foundation (Grant No. 8151018201000039), and the Student Innovation Ability Improvement Program of Guangzhou Medical University (2026–2027, No. S20261057156).

Institutional Review Board Statement: All animal procedures were reviewed and approved by the Animal Ethics Committee of Guangzhou Medical University (Approval No. GY2025–1023, approved on 14 May 2026). All procedures involving animals were conducted in accordance with institutional and national guidelines for the care and use of laboratory animals, with appropriate measures taken to minimise animal pain, distress, and unnecessary suffering.

Informed Consent Statement: Not applicable.

Data Availability Statement: The datasets generated and/or analysed during this study are available from the corresponding author upon request.

Conflicts of Interest: A patent application related to the oral orotracheal bronchoalveolar lavage device (OOBL) described in this study has been filed, with one or more authors named as inventors. The study also received financial support as disclosed in the Funding section. The authors declare no other conflicts of interest.

Abbreviations

BAL, bronchoalveolar lavage; BALF, bronchoalveolar lavage fluid; ELISA, enzyme-linked immunosorbent assay; H&E, hematoxylin and eosin; IL, interleukin; LPS, lipopolysaccharide; MPO, myeloperoxidase; OOBL, oral orotracheal bronchoalveolar lavage device; PBS, phosphate-buffered saline; qRT-PCR, quantitative reverse-transcription polymerase chain reaction; RBC, red blood cell; TC, total cell; TNF-α, tumour necrosis factor-α; TBL, tracheotomy-based lavage; WBC, white blood cell.

References

1. Poitout-Belissent, F.; Grant, S.N.; Tepper, J.S. Aspiration and Inspiration: Using Bronchoalveolar Lavage for Toxicity Assessment. *Toxicol. Pathol.* **2020**, *49*, 386–396. [CrossRef] [PubMed]
2. Maux, J.M.L.; Silva, H.G.; Silva, M.E.T.A.; Albuquerque, G.S.; Leão, G.J.M.; Silva, I.C.; Arruda, E.N.T.; Matos, T.C.N.; Caribé, C.F.C.; Silva-Neto, J.C. Use of bronchoalveolar lavage in the diagnosis of pulmonary diseases and its potential clinical-laboratory applications: A review. *Braz. J. Biol.* **2025**, *85*, e292731. [CrossRef] [PubMed]
3. Novoa-Bolivar, E.M.; Ros, J.A.; Pérez-Fernández, S.; Campillo, J.A.; López-Hernández, R.; González-López, R.; Ruiz–Lorente, I.; Otálora-Alcaraz, A.; Ortuño-Hernández, C.; Gimeno, L.; et al. Diagnostic Utility of Bronchoalveolar Lavage Flow Cytometric Leukocyte Profiling in Interstitial Lung Disease and Infection. *Biomolecules* **2025**, *15*, 597. [CrossRef] [PubMed]
4. Daubeuf, F.; Frossard, N. Performing Bronchoalveolar Lavage in the Mouse. *Curr. Protoc. Mouse Biol.* **2012**, *2*, 167–175. [CrossRef] [PubMed]
5. Van Hoecke, L.; Job, E.R.; Saelens, X.; Roose, K. Bronchoalveolar Lavage of Murine Lungs to Analyze Inflammatory Cell Infiltration. *J. Vis. Exp.* **2017**, *123*, e55398. [CrossRef] [PubMed]
6. Shen, R.; Jiang, Y.; Liu, G.; Gao, S.; Sun, H.; Wu, X.; Gu, J.; Wu, H.; Mo, K.; Niu, X.; et al. Single-Cell Landscape of Bronchoalveolar Lavage Fluid Identifies Specific Neutrophils during Septic Immunosuppression. *Adv. Sci.* **2025**, *12*, e2406218. [CrossRef] [PubMed]
7. Tisch, L.J.; Bartone, R.D.; Antoniak, S.; Bonner, J.C. Inhibition of protease-activated receptor-2 attenuates multi-walled carbon nanotube exacerbation of allergic lung disease in mice. *Part. Fibre Toxicol.* **2025**, *22*, 32. [CrossRef] [PubMed]
8. Mariappan, N.; Zafar, I.; Robichaud, A.; Wei, C.-C.; Shakil, S.; Ahmad, A.; Goymer, H.M.; Abdelsalam, A.; Kashyap, M.P.; Foote, J.B.; et al. Pulmonary pathogenesis in a murine model of inhaled arsenical exposure. *Arch. Toxicol.* **2023**, *97*, 1847–1858. [CrossRef] [PubMed]
9. Liu, Y.; Li, F.; Tang, L.; Pang, K.; Zhang, Y.; Zhang, C.; Guo, H.; Ma, T.; Zhang, X.; Yang, G.; et al. Extracellular mitochondria contribute to acute lung injury via disrupting macrophages after traumatic brain injury. *J. Neuroinflammation* **2025**, *22*, 63. [CrossRef] [PubMed]
10. Song, J.-A.; Yang, H.-S.; Lee, J.-S.; Kwon, S.-J.; Jung, K.-J.; Heo, J.-D.; Cho, K.-H.; Song, C.-W.; Lee, K.-H. Standardization of Bronchoalveolar Lavage Method Based on Suction Frequency Number and Lavage Fraction Number Using Rats. *Toxicol. Res.* **2010**, *26*, 203–208. [CrossRef] [PubMed]
11. Di, Y.P. Assessment of Pathological and Physiological Changes in Mouse Lung Through Bronchoalveolar Lavage. In *Methods in Molecular Biology*; Humana Press: Totowa, NJ, USA, 2014; pp. 33–42.
12. Peng, L.; Xu, W.; Wang, J.; Liu, Y.; Qian, W.; Wang, S.; Xie, T.; Shan, J. Optimization of bronchoalveolar lavage fluid volume for untargeted lipidomic method and application in influenza A virus infection. *J. Pharm. Biomed. Anal.* **2023**, *236*, 115677. [CrossRef] [PubMed]
13. Mancini, M.; Greco, A.; Tedeschi, E.; Palma, G.; Ragucci, M.; Bruzzone, M.G.; Coda, A.R.D.; Torino, E.; Scotti, A.; Zucca, I.; et al. Head and Neck Veins of the Mouse. A Magnetic Resonance, Micro Computed Tomography and High Frequency Color Doppler Ultrasound Study. *PLoS ONE* **2015**, *10*, e0129912. [CrossRef] [PubMed]
14. Kim, M.J.; Kim, Y.Y.; Chao, J.R.; Park, H.S.; Chang, J.; Oh, D.; Lee, J.J.; Kang, T.C.; Suh, J.; Lee, J.H. Comparing the Organs and Vasculature of the Head and Neck in Five Murine Species. *In Vivo* **2017**, *31*, 861–871. [CrossRef] [PubMed]
15. Luckow, B.; Lehmann, M.H. A Simplified Method for Bronchoalveolar Lavage in Mice by Orotracheal Intubation Avoiding Tracheotomy. *BioTechniques* **2021**, *71*, 534–537. [CrossRef] [PubMed]
16. Maxeiner, J.H.; Karwot, R.; Hausding, M.; Sauer, K.A.; Scholtes, P.; Finotto, S. A method to enable the investigation of murine bronchial immune cells, their cytokines and mediators. *Nat. Protoc.* **2007**, *2*, 105–112. [CrossRef] [PubMed]
17. Sasaki, K.; Ito, T.; Shiga, T.; Uemura, K.; Ishikawa, T. An evaluation of the feasibility of a transoral endotracheal intubation method in mice using a combination of commercially available research equipment. *J. Vet. Med. Sci.* **2025**, *87*, 589–593. [CrossRef] [PubMed]
18. Di, M.E.; Yang, D.; Di, Y.P. Using Bronchoalveolar Lavage to Evaluate Changes in Pulmonary Diseases. In *Methods in Molecular Biology*; Humana Press: Totowa, NJ, USA, 2020; pp. 117–128.
19. Zheng, L.; Liu, C.; Wang, H.; Zhang, J.; Mao, L.; Dong, X.; Hu, S.; Li, N.; Pi, D.; Qiu, J.; et al. Intact lung tissue and bronchoalveolar lavage fluid are both suitable for the evaluation of murine lung microbiome in acute lung injury. *Microbiome* **2024**, *12*, 56. [CrossRef] [PubMed]
20. Ritter, E.; Hohl, K.; Kereskai, L.; Kemény, Á.; Hargitai, D.; Szombati, V.; Perkecz, A.; Pakai, E.; Garami, A.; Zsembery, Á.; et al. Optimization, Characterization and Pharmacological Validation of the Endotoxin-Induced Acute Pneumonitis Mouse Model. *Biomedicines* **2025**, *13*, 1498. [CrossRef] [PubMed]
21. Deng, A.-X.; Zhao, L.; Ruze, A.; Li, Q.-L.; Zhao, B.-H.; Hu, S.; Gai, M.-T.; Wang, H.-L.; Yao, Q.-L.; Gao, X.-M. Application of ultrasound in assessment of acute lung injury in mice. *PLoS ONE* **2025**, *20*, e0332912. [CrossRef] [PubMed]

22. Fu, J.; Liu, Z.; Feng, Z.; Huang, J.; Shi, J.; Wang, K.; Jiang, X.; Yang, J.; Ning, Y.; Lu, F.; et al. Platycodon grandiflorum exosome-like nanoparticles: The material basis of fresh platycodon grandiflorum optimality and its mechanism in regulating acute lung injury. *J. Nanobiotechnology* **2025**, *23*, 270. [CrossRef] [PubMed]
23. Louis-Maerten, E.; Rodriguez Perez, C.; Cajiga, R.M.; Persson, K.; Elger, B.S. Conceptual foundations for a clarified meaning of the 3Rs principles in animal experimentation. *Anim. Welf.* **2024**, *33*, e37. [CrossRef] [PubMed]
24. Nosaka, N.; Crother, T.R.; Chen, S.; Arditi, M.; Shimada, K. Optimal tube length of orotracheal intubation for mice. *Lab. Anim.* **2019**, *53*, 79–83. [CrossRef] [PubMed]
25. Dharmadhikari, S.; Best, C.A.; King, N.; Henderson, M.; Johnson, J.; Breuer, C.K.; Chiang, T. Mouse Model of Tracheal Replacement with Electrospun Nanofiber Scaffolds. *Ann. Otol. Rhinol. Laryngol.* **2019**, *128*, 391–400. [CrossRef] [PubMed]
26. Pang, Y.-L.; Fang, S.-Y.; Cheng, T.-T.; Huang, C.-C.; Lin, M.-W.; Lam, C.-F.; Chen, K.-B. Viable Allogeneic Mitochondria Transplantation Improves Gas Exchange and Alveolar-Capillary Permeability in Rats with Endotoxin-Induced Acute Lung Injuries. *Int. J. Med. Sci.* **2022**, *19*, 1036–1046. [CrossRef] [PubMed]
27. Schnitzerlein, M.; Greto, E.; Wegner, A.; Möller, A.; Aust, O.; Ben Brahim, O.; Blumenthal, D.B.; Zaburdaev, V.; Uderhardt, S. Cellular morphodynamics as quantifiers for functional states of resident tissue macrophages in vivo. *PLoS Comput. Biol.* **2025**, *21*, e1011859. [CrossRef]
28. Zhang, Y.; Zheng, W.; Ning, H.; Liu, J.; Li, F.; Ju, X. Interleukin-6 in blood and bronchoalveolar lavage fluid of hospitalized children with community-acquired pneumonia. *Front. Pediatr.* **2022**, *10*, 922143. [CrossRef] [PubMed]
29. Voiriot, G.; Dorgham, K.; Bachelot, G.; Fajac, A.; Morand-Joubert, L.; Parizot, C.; Gerotziafas, G.; Farabos, D.; Trugnan, G.; Eguether, T.; et al. Identification of bronchoalveolar and blood immune-inflammatory biomarker signature associated with poor 28-day outcome in critically ill COVID-19 patients. *Sci. Rep.* **2022**, *12*, 9502. [CrossRef] [PubMed]
30. Fröhlich, E.; Loizou, G.D. Editorial: 3Rs—Strategies for reduction and refinement of animal studies. *Front. Pharmacol.* **2023**, *14*, 1200965. [CrossRef] [PubMed]

Disclaimer/Publisher's Note: The statements, opinions and data contained in all publications are solely those of the individual author(s) and contributor(s) and not of MDPI and/or the editor(s). MDPI and/or the editor(s) disclaim responsibility for any injury to people or property resulting from any ideas, methods, instructions or products referred to in the content.